




ORIGINAL ARTICLE

HSP90/IKK-rich small extracellular vesicles activate pro-angiogenic melanoma-associated fibroblasts via the NF- κ B/CXCL1 axis

Hokeung Tang¹  | Xiaocheng Zhou² | Xiaoping Zhao³ | Xinyue Luo¹  | Tingting Luo⁴ | Yang Chen¹ | Weilian Liang¹ | Erhui Jiang⁵ | Ke Liu⁵ | Zhe Shao⁵  | Zhengjun Shang⁵

¹The State Key Laboratory Breeding Base of Basic Science of Stomatology (Hubei-MOST) & Key Laboratory for Oral Biomedicine Ministry of Education, School and Hospital of Stomatology, Wuhan University, Wuhan, China

²Department of Oral and Maxillofacial Surgery, School and Hospital of Stomatology, Wuhan University, Wuhan, China

³Center of Stomatology, Tongji Hospital, Tongji Medical College, Huazhong University of Science and Technology, Wuhan, China

⁴Shenzhen PKU-HKUST Medical Center (Peking University Shenzhen Hospital), Shenzhen, China

⁵Department of Oral and Maxillofacial-Head and Neck Oncology, School and Hospital of Stomatology, Wuhan University, Wuhan, China

Correspondence

Zhe Shao and Zhengjun Shang, The State Key Laboratory Breeding Base of Basic Science of Stomatology (Hubei-MOST) & Key Laboratory for Oral Biomedicine Ministry of Education & Department of Oral and Maxillofacial-Head and Neck Oncology, School and Hospital of Stomatology, Wuhan University, 430079 Wuhan, China.

Emails: shaozhe@whu.edu.cn (Z. S.) and shangzhengjun@whu.edu.cn, (Z. S.)

Funding information

Xiaocheng Zhou, Grant/Award Number: 2042020kf0176; Zhengjun Shang, Grant/Award Number: 81672666 and 81972547

Abstract

Hypoxia is a main feature of most solid tumors, but how melanoma cells under hypoxic conditions exploit tumor microenvironment (TME) to facilitate tumor progression remains poorly understood. In this study, we found that hypoxic melanoma-derived small extracellular vesicles (sEVs) could improve the proangiogenic capability of cancer-associated fibroblasts (CAFs). This improvement was due to the activation of the IKK/I κ B/NF- κ B signaling pathway and upregulation of CXCL1 expression and secretion in CAFs. By proteomic analysis, we verified that hypoxia could promote enrichment of chaperone HSP90 and client protein phosphorylated IKK α / β (p-IKK α / β) in melanoma-derived sEVs. Delivery of the HSP90/p-IKK α / β complex by sEVs could activate the IKK/I κ B/NF- κ B/CXCL1 axis in CAFs and promote angiogenesis in vitro and in vivo. Taken together, these findings deepen the understanding of hypoxic response in melanoma progression and provide potential targets for melanoma treatment.

KEYWORDS

angiogenesis, cancer-associated fibroblasts, extracellular vesicles, hypoxia, melanoma

Abbreviations: 17-AAG, tanesipimycin; APDC, pyrrolidinedithiocarbamate ammonium; CAFs, cancer-associated fibroblasts; CCK-8, Cell Counting Kit-8; CM, conditioned medium; Co-IP, coimmunoprecipitation; CXCL1, C-X-C motif chemokine ligand 1; DMSO, dimethyl sulfoxide; ELISA, enzyme-linked immunosorbent assay; FAP, fibroblast activation protein; FBS, fetal bovine serum; H, hypoxic; HNSCC, head and neck squamous cell carcinoma; HPLC, high-performance liquid chromatography; HSP90AA1, heat shock protein 90 alpha, class A member 1; HSP90AB1, heat shock protein 90 alpha, class B member 1; HUVECs, human umbilical vein endothelial cells; i.p., intraperitoneal injection; IF, immunofluorescence; IHC, immunohistochemistry; MEM-EBSS, minimum essential medium Eagle's with Earle's balanced salts; MVD, microvessel density; N, normoxic; NS, not significant; PBS, phosphate buffer solution; p-IKK α / β , phosphorylated IKK α / β ; p-I κ B α , phosphorylated I κ B α ; PVDF, polyvinylidene difluoride; RPMI, Roswell Park Memorial Institute; SDS-PAGE, sodium dodecyl sulfate polyacrylamide gel; SEM, standard error of the mean; sEV, small extracellular vesicle; TEM, transmission electron microscopy; TME, tumor microenvironment; TSG101, tumor susceptibility gene 101; α -SMA, α -smooth muscle actin.

Hokeung Tang, Xiaocheng Zhou, and Xiaoping Zhao contributed equally to this work.

This is an open access article under the terms of the Creative Commons Attribution-NonCommercial License, which permits use, distribution and reproduction in any medium, provided the original work is properly cited and is not used for commercial purposes.

© 2022 The Authors. *Cancer Science* published by John Wiley & Sons Australia, Ltd on behalf of Japanese Cancer Association.

1 | INTRODUCTION

Melanoma is a highly aggressive malignant tumor with intense invasiveness and angiogenesis. Although multiple-targeted therapies have been validated in antitumor treatment, the prognosis for melanoma patients still remains unoptimistic, especially for those who relapse.¹ Accumulating evidence indicates that TME plays vital roles in tumor proliferation, angiogenesis, metastasis, and drug resistance. Within TME, CAFs are major stromal cells that act as the pivotal contributor to tumor progression.² However, how melanoma cells manipulate CAFs to foster tumor progression still remains obscure. Unraveling the mechanisms of cross talk between melanoma cells and CAFs could provide potential targets for oncotherapy.

In recent years, sEVs (≤ 200 nm) have drawn much attention in intercellular communication. Carrying numerous bioactive cargos, tumor-derived sEVs orchestrate TME and contribute to tumor progression.³ But how melanoma-derived sEVs reprogram CAFs to promote tumor progression remains poorly understood.

Hypoxia is a critical feature of most solid tumors and promotes tumor invasion, angiogenesis, and drug resistance. Hypoxia also promotes sEV secretion from tumor cells and changes the cargos of sEVs. With enrichment of hypoxia-related cargos, hypoxic tumor cell-derived sEVs modify the TME and play key roles in tumor angiogenesis, immunomodulation, and drug resistance.⁴ However, the effects and mechanisms of hypoxic melanoma-derived sEVs on CAF reprogramming are ill defined.

Our previous study has verified that melanoma-derived exosomal miR-155-5p could induce the proangiogenic switch of CAFs and promote tumor angiogenesis.⁵ In this study, we aimed to investigate the potential effects and mechanisms of hypoxic melanoma-derived sEVs on CAF reprogramming.

2 | MATERIALS AND METHODS

2.1 | Reagents

Details are described in the Supplemental Materials and Methods.

2.2 | Cell lines and culture

Details are described in the Supplemental Materials and Methods.

2.3 | Small extracellular vesicle isolation and identification

For sEV isolation, B16, B16F10, and A375 cells at 80% cell density were washed thrice with PBS and then cultured with the corresponding culture medium without FBS at 37°C in 5% CO₂ and 20% O₂ or 37°C in 5% CO₂ and 1% O₂. After 24 hours, the supernatant was collected and precleared by sequential centrifugation at 300 g

(10 minutes), 2000 g (10 minutes), and 10 000 g (30 minutes). All kinds of sEVs were isolated by ultracentrifugation at 120,000 g for 70 minutes (conducted with Optima XE-100 ultracentrifuge, Beckman Coulter) and suspended in PBS. Small extracellular vesicle were observed by transmission electron microscopy HT7700 (HITACHI). The hydrodynamic diameter of sEVs was measured by Zetasizer Nano-ZS90 (Malvern Instruments).

2.4 | Small extracellular vesicle tracing

The sEVs were labeled with PKH26 and CFSE (Sigma-Aldrich) following the manufacturer's instructions. After incubation for 4 hours, the uptake of PKH26- and CFSE-labeled sEVs by HFF-1 cells was observed by confocal microscopy (Olympus FV1200).

2.5 | RNA-seq analysis

Details are described in the Supplemental Materials and Methods.

2.6 | Proteomic analysis

Details are described in the Supplemental Materials and Methods.

2.7 | Protein extraction and Western blot analysis

Details are described in the Supplemental Materials and Methods.

2.8 | Small extracellular vesicle membrane and cytosol isolation assay

Details are described in the Supplemental Materials and Methods.

2.9 | Enzyme-linked immunosorbent assay

The concentration of CXCL1 in the CM was detected by ELISA kits (EK0722, Boster Biological Technology) following the manufacturer's instructions and determined by comparing the optical densities at 450 nm with the standard curve of the kits.

2.10 | Migration and tube formation assay

When HFF-1 cell density reached 70%-80%, A375-derived sEVs were added to the medium at 20 μ g/mL. After 24 hours, the CM was collected and prepared for further experiments. For scratch assay, a scratch was made in each well after the cells had formed confluent monolayer. After the cells had been washed three times with PBS,

HUVECs were incubated with the corresponding CM to estimate the migration ability. Digital images were taken at 0 and 24 hours after the scratches by microscope (BHS-313 Olympus). In tube formation assay, HUVECs (1×10^4 /well) were seeded in 48-well plates

precoated with Matrigel (BD Biosciences) and cultured in the CM from sEV-treated HFF-1 cells. The capillary-like structure was observed and photographed after 6 hours of incubation. Quantification and analysis of migration and tube formation results were assessed

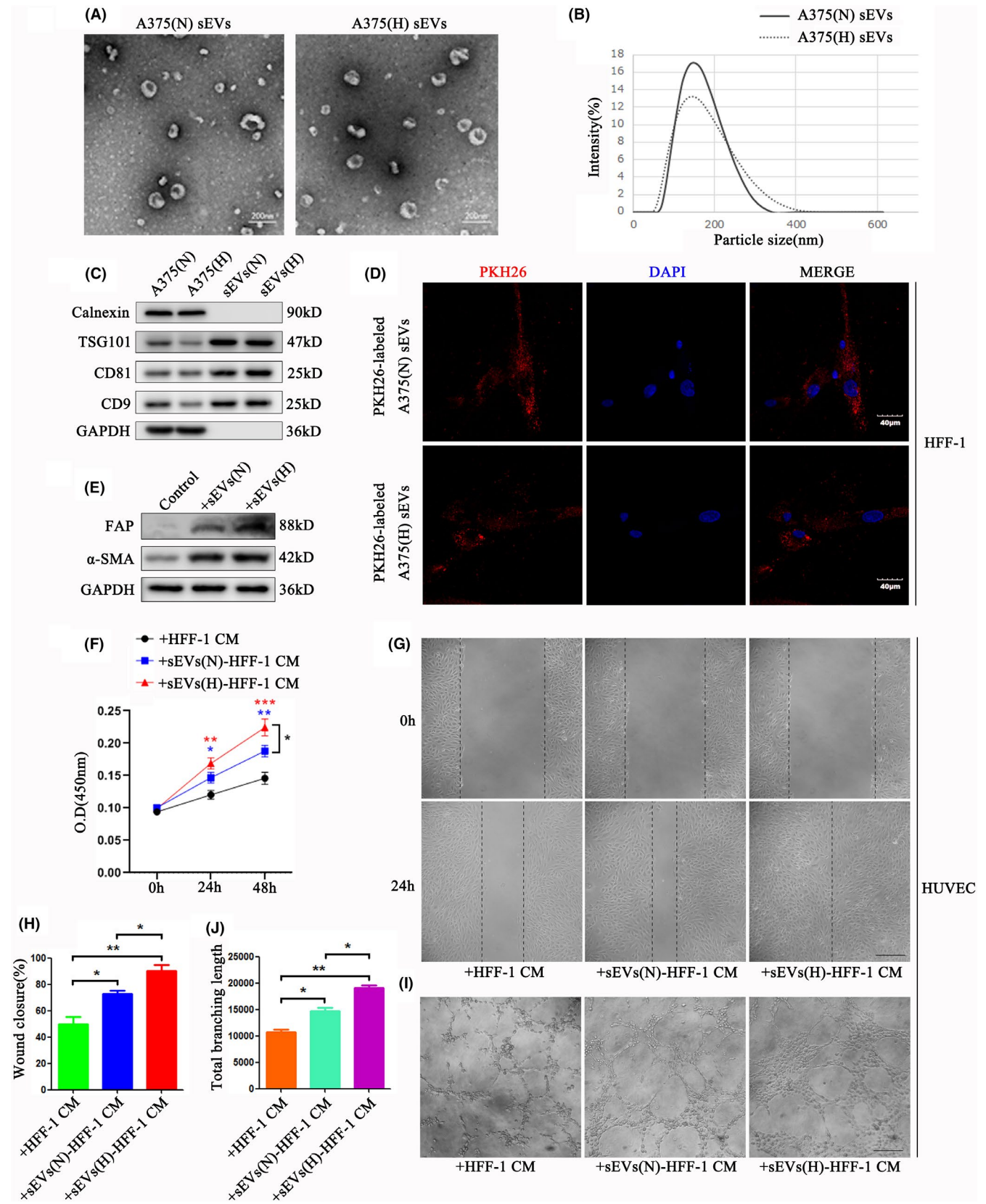


FIGURE 1 Hypoxic melanoma-derived small extracellular vesicles (sEVs) enhance the proangiogenic capability of cancer-associated fibroblasts (CAFs). Small extracellular vesicles secreted by normoxic and hypoxic A375 cells were identified by TEM (A) and dynamic light-scattering analysis (B). Scale bar: 200 nm. N, normoxic; H, hypoxic. C, Protein markers of sEVs (TSG101, CD9, and CD81) and endoplasmic reticulum (calnexin) were detected by Western blot. D, The uptake of PKH26-labeled A375 sEVs by HFF-1 cells was investigated by confocal microscope. Scale bar: 40 μ m. E, The expression of CAF markers (FAP and α -SMA) in HFF-1 cells was examined by Western blot after different treatments for 24 h. GAPDH was used as the internal control. Cell Counting Kit-8 proliferation assay (F), scratch assay (G, H), and tube formation assay (I, J) investigated the effects of conditioned medium (CM) from HFF-1 cells, normoxic A375 sEV-treated HFF-1 cells, and hypoxic A375 sEV-treated HFF-1 cells on HUVEC proliferation, migration, and tube formation. Scale bar: 50 μ m. Independent experiments were performed in triplicate. * $P < .05$, ** $P < .01$, *** $P < .001$; Student's t tests. Values represent means \pm SEM

by using Image-Pro Plus 6.0 (Media Cybernetics). Both assays above were replicated three times.

2.11 | Cell proliferation assay

Human umbilical vein endothelial cells were seeded in 96-well culture plates and cultured by the CM of fibroblasts, which were stimulated with or without A375-secreted sEVs. After incubation for 24 and 48 hours, cell proliferation was determined by CCK-8 (C0037, Beyotime) according to the manufacturer's instructions.

2.12 | Coimmunoprecipitation assay

Coimmunoprecipitation was performed by using Universal Magnetic Co-IP kits (54 002, Active Motif). A375-derived sEVs were lysed following the manufacturer's instructions of the kit. A total of 5 μ g of HSP90AA1 antibody and HSP90AB1 antibody per sample was used for protein pulldown. The immunoprecipitated proteins were used for electrophoresis and transfer steps as described above. The presence of immunoprecipitated p-IKK α/β was determined by Western blot.

2.13 | Chromatographic and mass spectrometric analysis

Details are described in the Supplemental Materials and Methods.

2.14 | In vivo study

The experimental procedures were approved by the Laboratory Animal Care and Use Committee of Wuhan University (approval number: S07921010L). Twenty-five clean specific pathogen-free BALB/C nude mice (male, 6 weeks old) were purchased from Beijing Weitong Lihua Experimental Animal Technology Co., Ltd. The nude mice were raised in laminar flow cabinets under specific pathogen-free conditions with a 12 h light-dark cycle. A375 cells (5×10^5) and HFF-1 cells (5×10^5) were mixed with Matrigel (100 μ L) and subcutaneously injected into the right back of every nude mouse. Two days later, the size of the xenografts was measured

every day and calculated with the formula: volume (cm^3) = (width² \times length) / 2. Two days after the first measurement, the mice were divided into five groups (five mice each group) and subjected to various treatments. Groups were set up at the first treatment as follows: (a) vehicle solution, i.p.; saline, intratumorally; (b) vehicle solution, i.p.; sEVs(N), intratumorally; (c) 17-AAG (50 mg/kg), i.p.; sEVs(N), intratumorally; (d) vehicle solution, i.p.; sEVs(H), intratumorally; (e) 17-AAG (50 mg/kg), i.p.; sEVs(H), intratumorally. After the first treatment, groups were set up as follows with treatment every 2 days: (a) vehicle solution, i.p.; (b) vehicle solution, i.p.; (c) 17-AAG (50 mg/kg), i.p.; (d) vehicle solution, i.p.; (e) 17-AAG (50 mg/kg), i.p. The vehicle solution was 5% DMSO, 40% PEG300, 5% Tween-80, and 50% saline. After 9 days, xenografts were harvested for further analyses.

2.15 | Immunohistochemistry and immunofluorescence

The xenografts were fixed in 4% paraformaldehyde for 24 hours and then embedded in paraffin and serially sectioned (4 μ m). For IHC, the specimens were incubated with α -SMA, fibronectin, and CXCL1 antibodies overnight at 4°C and then detected by using the UltrasensitiveTM SP (Mouse/Rabbit) IHC kits (KIT-9710, MXB) and DAB kits (DAB-0031, MXB). Hematoxylin was used to stain the nucleus. The staining intensity was classified into four levels: negative (0), weak (1), moderate (2), and strong (3). The staining extent was also classified into four levels: 1 ($\leq 25\%$), 2 (25%-50%), 3 (51%-75%), and 4 ($> 75\%$). Immunohistochemistry score was calculated by multiplying the two levels together. For IF, the specimens were incubated with CD31 antibody overnight at 4°C and then with Cy3-conjugated IgG. Analyses were performed with a fluorescent microscope (Biozero BZ-8000, Keyence). Microvessel density was counted from six random microscopic fields.

2.16 | Statistical analysis

All the results are expressed as means \pm SEM from triplicates of independent experiments and analyzed by student's t tests or one-way ANOVA by using the GraphPad Prism software. Statistical significance of the results was verified when $P < .05$.

3 | RESULTS

3.1 | Hypoxic melanoma-derived sEVs enhance the proangiogenic capability of CAFs in vitro

In this study, sEVs were isolated from the culture supernatant of human melanoma cell line A375 cells cultured under normoxic and hypoxic conditions. Both normoxic and hypoxic sEVs exhibited cup and biconcave morphology (Figure 1A). TEM and dynamic light scattering analysis revealed that the diameter of most particles was below 200 nm (Figure 1A,B). Besides, the presence of sEV markers (TSG101, CD9, and CD81) and absence of an endoplasmic reticulum marker (calnexin) confirmed the existence and purity of sEVs as shown by Western blot (Figure 1C, Figure S1).

Our previous studies indicated that melanoma-derived sEVs could convert fibroblasts into CAFs.^{5,6} In this study, the normoxic and hypoxic sEVs were fluorescently labeled with PKH26 and added to the culture medium of HFF-1 fibroblasts. After 12 hours of incubation, the cytosol of HFF-1 cells was fluorescently stained, confirming the uptake of sEVs by HFF-1 cells (Figure 1D). Treatment with sEVs significantly upregulated CAF marker expression (FAP and α -SMA) in HFF-1 cells, indicating that both normoxic and hypoxic melanoma-derived sEVs could transform fibroblasts into CAFs (Figure 1E).

We had found that melanoma-derived exosomes could induce the proangiogenic switch of CAFs.⁵ However, the effects of hypoxic melanoma-derived sEVs on the proangiogenic capability of CAFs were still unclear. In this study, we used the CM from normoxic and hypoxic sEV-treated HFF-1 cells to cultivate HUVECs. Cell-Counting Kit-8 proliferation assay showed that the CM of hypoxic sEV-treated HFF-1 cells promoted HUVEC proliferation more efficiently than the normoxic counterpart (Figure 1F). Furthermore, scratch assay and tube formation assay revealed that the CM of hypoxic sEV-treated HFF-1 cells was more potent than the normoxic counterpart to promote HUVEC migration and tube formation (Figure 1G-J).

3.2 | Hypoxic melanoma-derived sEVs improve the proangiogenic capability of CAFs by upregulating CXCL1 expression

To investigate mechanisms underlying the hypoxic sEV-induced proangiogenic capability improvement of CAFs, transcriptome of

HFF-1 cells and sEV-treated HFF-1 cells was compared by RNA-seq analysis. We searched every target among the markedly up-regulated genes in the PubMed database (Figure 2A) and found large amounts of reports revealing the proangiogenic capability of CXCL1.⁷⁻⁹ Besides, there were few reports linking other up-regulated molecules (especially FAM86B2, GOLGA8Q, RIMBP3C, CD302, PCDHB11, and MOB4) with angiogenesis. CXCL1 was significantly upregulated in normoxic and hypoxic sEV-treated HFF-1 cells. Meanwhile, the CXCL1 level was much higher in hypoxic sEV-treated HFF-1 cells than the normoxic counterpart (Figure 2A). Western blot and ELISA verified that CXCL1 expression and secretion levels were obviously upregulated in normoxic sEV-treated HFF-1 cells and even higher in hypoxic sEV-treated HFF-1 cells (Figure 2B,C). Therefore, we hypothesized that CXCL1 played a crucial role in hypoxic sEV-induced proangiogenic capability improvement of CAFs. To verify this hypothesis, we added CXCL1 antibody into the CM of sEV-treated HFF-1 cells to block active CXCL1 (Figure 2D, Figure S2), and then used this CM to cultivate HUVECs. Cell-Counting Kit-8 proliferation assay, scratch assay, and tube formation assay revealed that blocking CXCL1 in the CM of sEV-treated HFF-1 cells remarkably inhibited HUVEC proliferation, migration, and tube formation (Figure 2E-H).

3.3 | Melanoma-derived sEVs regulate CXCL1 expression and the proangiogenic capability of CAFs through IKK/I κ B/NF- κ B signaling pathway

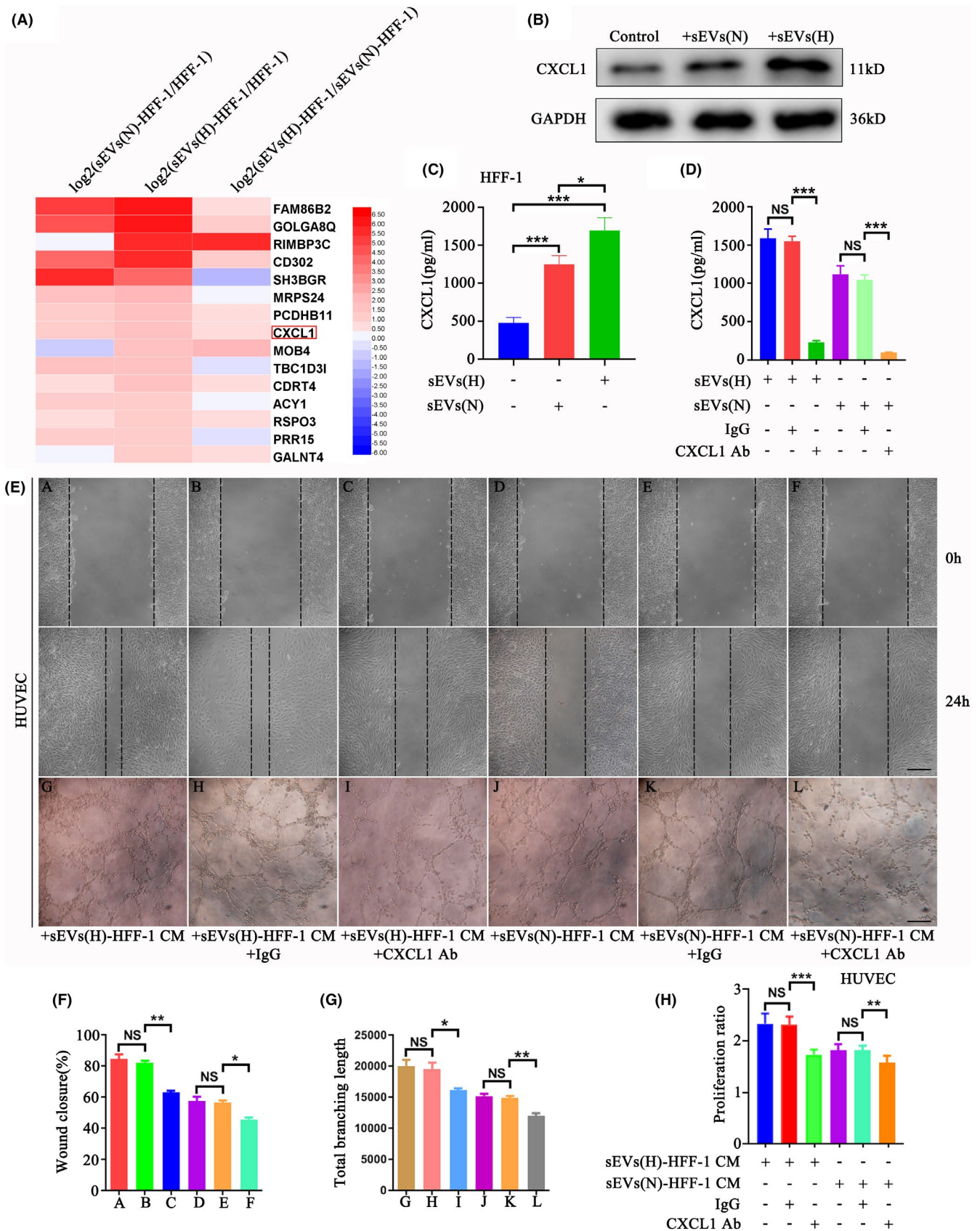
How melanoma-derived sEVs regulate chemokine expression in CAFs was not fully understood. As the NF- κ B pathway was found to participate in hypoxic response and chemokine regulation in tumor cells,¹⁰ we investigated whether the NF- κ B pathway regulated sEV-induced CXCL1 expression in CAFs. Western blot showed that treatment of A375-secreted sEVs, especially hypoxic A375-secreted sEVs, significantly elevated p-IKK α / β , p-I κ B α , NF- κ B, and CXCL1 levels in HFF-1 cells (Figure 3A). However, APDC, an NF- κ B pathway inhibitor, significantly reduced p-IKK α / β , p-I κ B α , NF- κ B, and CXCL1 levels in sEV-treated HFF-1 cells (Figure 3B). Moreover, APDC remarkably downregulated CXCL1 secretion from sEV-treated HFF-1 cells (Figure 3C).

To explore the effects of the NF- κ B pathway on the proangiogenic capability of CAFs, we stimulated sEV-treated HFF-1 cells

FIGURE 2 Hypoxic melanoma-derived small extracellular vesicles (sEVs) improve the proangiogenic capability of cancer-associated fibroblasts (CAFs) by upregulating CXCL1 expression. A, The transcriptome in HFF-1 cells treated with normoxic and hypoxic A375 sEVs was detected by RNA-seq analysis. The gene expression levels in different groups were compared and ranked by ratio. The heat map exhibited the top upregulated genes. N, normoxic; H, hypoxic. B, C, CXCL1 expression and secretion levels in HFF-1 cells treated with normoxic and hypoxic A375 sEVs were investigated by Western blot and ELISA. The conditioned medium (CM) of A375 sEV-treated HFF-1 cells was collected and mixed with IgG and CXCL1 antibody. D, CXCL1 antibody significantly blocked active CXCL1 in the CM of A375 sEV-treated HFF-1 cells. Effects of the CM on HUVEC proliferation, migration, and tube formation was examined by CCK-8 assay (H), scratch assay (E, F), and tube formation assay (E, G). In CCK-8 assay, proliferation levels of HUVECs at 0 h were used as control. Proliferation levels at 48 h are presented. Ab, antibody. Scale bar: 50 μ m. Independent experiments were performed in triplicate. NS, not significant. * $P < .05$, ** $P < .01$, *** $P < .001$; Student's *t* tests. Values represent means \pm SEM

with APDC and then collected the CM to cultivate HUVECs. Cell Counting Kit-8 proliferation assay, scratch assay, and tube formation assay showed that the APDC treatment significantly alleviated

the promoting effects of CM collected from sEV-treated HFF-1 cells on HUVEC proliferation, migration, and tube formation (Figure 3D-G).



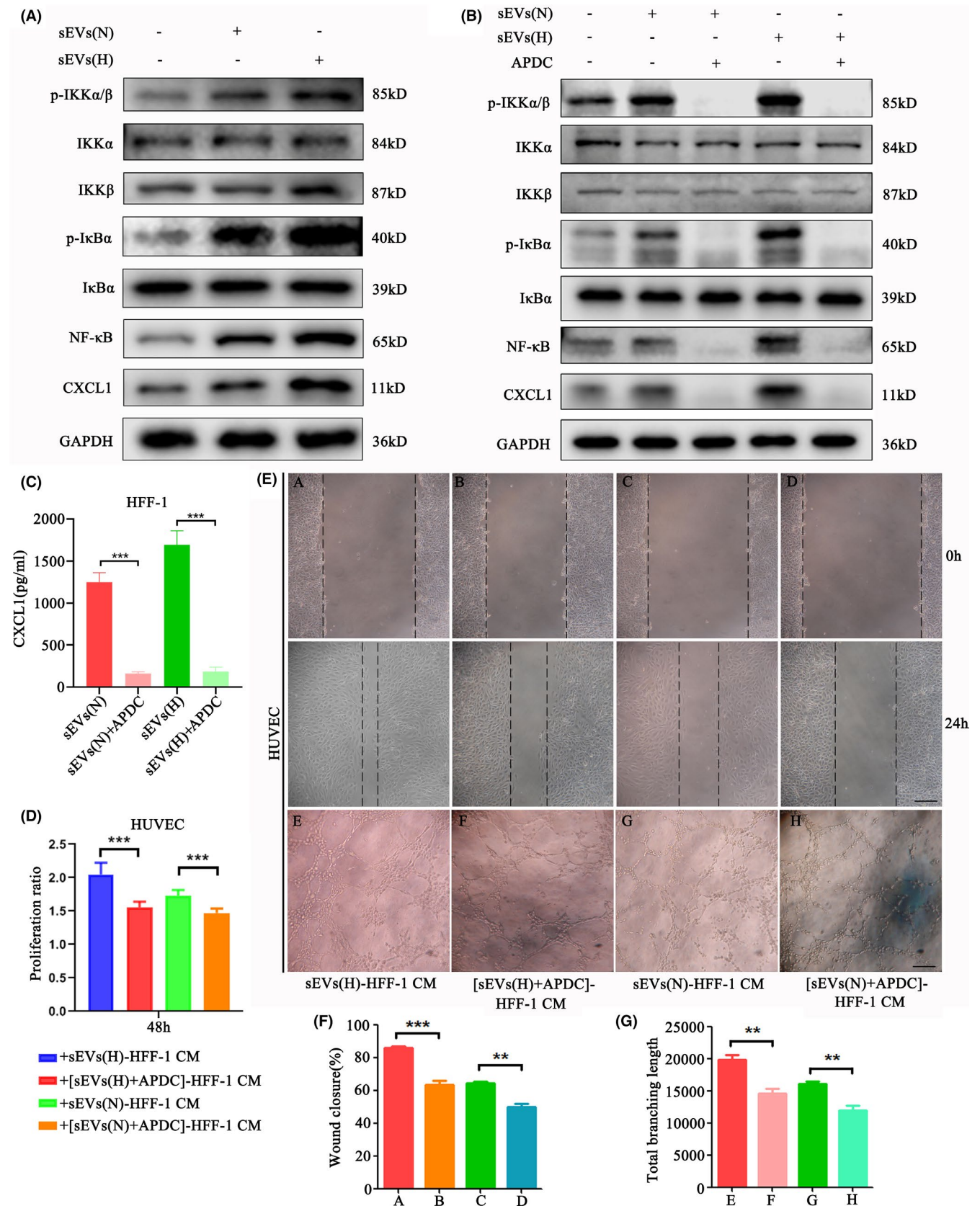


FIGURE 3 Melanoma-derived small extracellular vesicles (sEVs) regulate CXCL1 expression and the proangiogenic capability of cancer-associated fibroblasts (CAFs) through the IKK/I κ B/NF- κ B signaling pathway. A, B, P-IKK α/β , p-I κ B α , NF- κ B, and CXCL1 levels were upregulated in HFF-1 cells after sEV treatment and downregulated by APDC. GAPDH was used as the internal control. C, APDC inhibited CXCL1 secretion from sEV-treated HFF-1 cells. The APDC treatment significantly reduced the promoting effects of the conditioned medium (CM) from sEV-treated HFF-1 cells on HUVEC proliferation (D), migration (E, F), and tube formation (E, G). N, normoxic; H, hypoxic. Scale bar: 50 μ m. Independent experiments were performed in triplicate. ** $P < .01$, *** $P < .001$, Student's t tests. Values represent means \pm SEM

3.4 | Hypoxia promotes the enrichment of HSP90/p-IKK α / β complex in melanoma-derived sEVs

We had found that exosomal transfer of miR-155-5p from melanoma B16 and B16F10 cells to CAFs could induce the proangiogenic switch of CAFs.⁵ As B16 was a low-metastatic melanoma cell line while B16F10 was high metastatic, we used proteomic analysis to compare normoxic and hypoxic sEVs isolated from both cells. In virtue of the NCBI gene database and STRING v11 database,¹¹ we searched every top upregulated molecule from proteome analyses and discovered that chaperone HSP90AA1 had a close association with the IKK/ β /NF- κ B signaling pathway and exhibited higher levels in hypoxic sEVs and high-metastatic melanoma-derived sEVs (Figure 4A, B). Meanwhile, HSP90 subtype HSP90AB1 was also closely associated with the IKK/ β /NF- κ B signaling pathway (Figure 4B). Western blot verified that hypoxic A375-derived sEVs contained higher levels of HSP90AA1 and HSP90AB1 than normoxic A375-derived sEVs (Figure 4C). It was found that p-IKK α / β could be the client protein of HSP90.¹² In our study, Western blot confirmed the presence of p-IKK α / β in A375-derived sEVs and higher level of p-IKK α / β in hypoxic A375-derived sEVs (Figure 4C). Specifically, p-IKK α / β could be detected in the cytosol, but not on the membrane of A375-derived sEVs (Figure 4D). Moreover, HSP90 inhibitor 17-AAG dramatically reduced p-IKK α / β levels in normoxic and hypoxic A375-derived sEVs (Figure 4E). Furthermore, the results of Co-IP analysis confirmed that p-IKK α / β bonded chaperones HSP90AA1 and HSP90AB1 in normoxic and hypoxic A375-derived sEVs. Pretreating sEVs with 17-AAG inhibited the bond between p-IKK α / β and HSP90 (Figure 4F, Figure S3). These results indicated that hypoxia could promote the enrichment of the HSP90/p-IKK α / β complex in melanoma-derived sEVs.

3.5 | Melanoma-derived sEVs activate the IKK/ β /NF- κ B/CXCL1 axis and enhance the proangiogenic capability of CAFs by delivering the HSP90/p-IKK α / β complex

Treatment with normoxic and hypoxic A375-derived sEVs elevated HSP90 and p-IKK α / β levels in HFF-1 cells (Figure 5A). To clarify the effects of the HSP90/p-IKK α / β complex delivered by melanoma-derived sEVs on IKK/ β /NF- κ B/CXCL1 axis in CAFs, normoxic and hypoxic A375-derived sEVs were preincubated with 200 nM (0.117 μ g/mL) 17-AAG and then isolated to treat HFF-1 cells. The fluorescently stained cytoplasm of HFF-1 cells verified the uptake of 17-AAG-pretreated PKH26- and CFSE-labeled sEVs (Figure S4, Video S1 and S2). Western blot showed that pretreating sEVs with 17-AAG significantly reduced p-IKK α / β , p-I κ B α , NF- κ B, and CXCL1 levels in sEV-treated HFF-1 cells (Figure 5B). Pretreating sEVs with 17-AAG also remarkably reduced CXCL1 secretion in sEV-treated HFF-1 cells (Figure 5C). Furthermore, we performed HPLC and mass spectrometry to measure the concentration of 17-AAG in the 17-AAG-pretreated sEVs. The results revealed that

the mean concentration of 17-AAG was 0.0017 μ g/mL in normoxic sEVs and 0.0066 μ g/mL in hypoxic sEVs (Figure S5A, B). To investigate whether the carryover of 17-AAG in sEVs would obviously inhibit the IKK/ β /NF- κ B/CXCL1 pathway in HFF-1 cells, we assumed that the concentration of carryover reached 0.008 μ g/mL and used 0.008 μ g/mL 17-AAG to stimulate HFF-1 cells. Western blot revealed that 0.008 μ g/mL 17-AAG could not apparently inhibit the IKK/ β /NF- κ B/CXCL1 pathway in HFF-1 cells (Figure S5C, D). Indeed, at least part of 17-AAG firmly bonded HSP90 in sEVs, so the actual concentration of dissociative 17-AAG in sEVs was even less. Therefore, the influence of carryover of 17-AAG in sEVs on the IKK/ β /NF- κ B/CXCL1 pathway in HFF-1 cells could be ignored. These results indicated that the delivery of the HSP90/p-IKK α / β complex by melanoma-derived sEVs was able to activate the IKK/ β /NF- κ B/CXCL1 axis in CAFs.

Furthermore, we used the CM of HFF-1 cells which were treated with sEVs and 17-AAG-pretreated sEVs to cultivate HUVECs. In CCK-8 proliferation assay, scratch assay, and tube formation assay, HUVEC proliferation, migration, and tube formation levels apparently declined in the groups in which sEVs were pretreated with 17-AAG (Figure 5D-G).

3.6 | Blocking HSP90 impairs the promoting effects of sEVs on melanoma angiogenesis and progression in vivo

To explore the functions of melanoma-derived sEVs and HSP90 in vivo, xenograft models were set up. As Figure 6A-C showed, tumor masses grew larger and heavier in the groups treated with normoxic and hypoxic A375-derived sEVs. Besides, tumor masses in the hypoxic sEV-treated group were heavier and larger than those in the normoxic sEV-treated group. Intriguingly, application of 17-AAG significantly decreased tumor weight and size of xenografts. Furthermore, IHC analysis showed that treatment with sEVs upregulated α -SMA and CXCL1 expression in fibroblasts (fibronectin-positive districts). But 17-AAG potently inhibited α -SMA and CXCL1 expression in fibroblasts within the TME (Figure 6D-F, Figure S6). Moreover, treatment with sEVs increased the MVD of xenografts, but 17-AAG notably lowered the MVD (Figure 6G, H).

4 | DISCUSSION

Our previous study revealed that melanoma-derived exosomes could induce the proangiogenic switch of CAFs,⁵ but the roles and underlying mechanisms of hypoxic melanoma-derived sEVs in CAF modulation remained poorly understood. Here, we found that hypoxic stress could promote the enrichment of the HSP90/p-IKK α / β complex in melanoma-derived sEVs; sEVs derived from melanoma cells especially hypoxic melanoma cells could activate the IKK/ β /NF- κ B/CXCL1 axis in CAFs; and elevated CXCL1 secretion from CAFs was able to promote tumor angiogenesis and

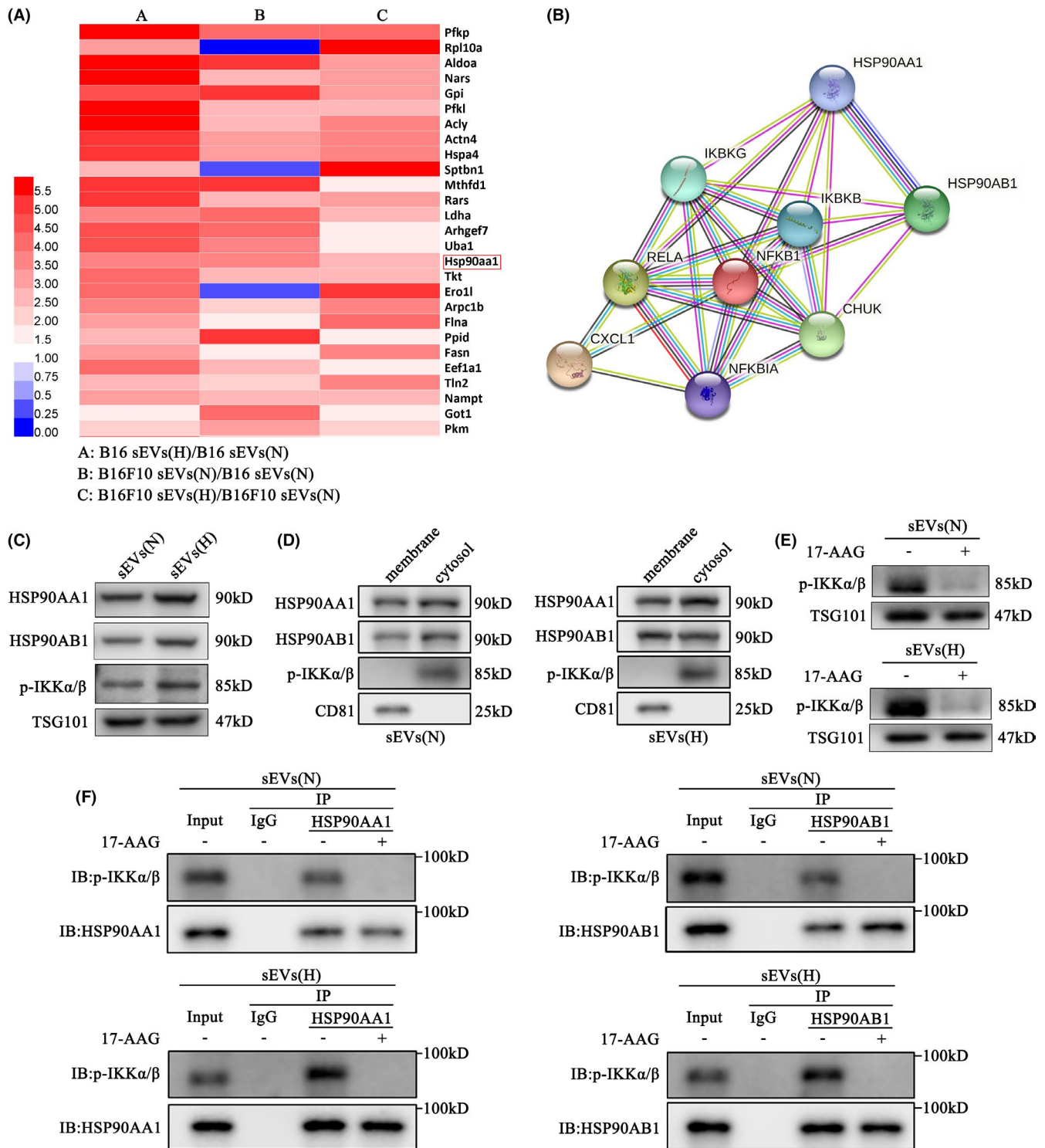


FIGURE 4 Hypoxia promotes the enrichment of the HSP90/p-IKK α/β complex in melanoma-derived small extracellular vesicles (sEVs). A, The ratio of protein levels as hypoxic sEVs versus normoxic sEVs and B16-derived sEVs versus B16F10-derived sEVs was ranked, and the top shared upregulated proteins were exhibited as heat map. B, The correlation between HSP90 subtypes and the IKK/I κ B/NF- κ B/CXCL1 pathway was obtained from the STRING v11 database. C, HSP90AA1, HSP90AB1, and p-IKK α/β levels in normoxic and hypoxic A375-derived sEVs was detected by Western blot. TSG101 was used as the internal control. D, P-IKK α/β could be detected in the cytosol but not on the membrane of normoxic and hypoxic A375-derived sEVs. CD81 was used as the marker of sEV membrane. E, 17-AAG dephosphorylated p-IKK α/β in normoxic and hypoxic A375-derived sEVs. F, Coimmunoprecipitation (Co-IP) analysis showed that p-IKK α/β bonded chaperones HSP90AA1 and HSP90AB1 in normoxic and hypoxic A375-derived sEVs, and pretreating sEVs with 17-AAG inhibited the bond between p-IKK α/β and HSP90. N, normoxic; H, hypoxic. Independent experiments were performed in triplicate

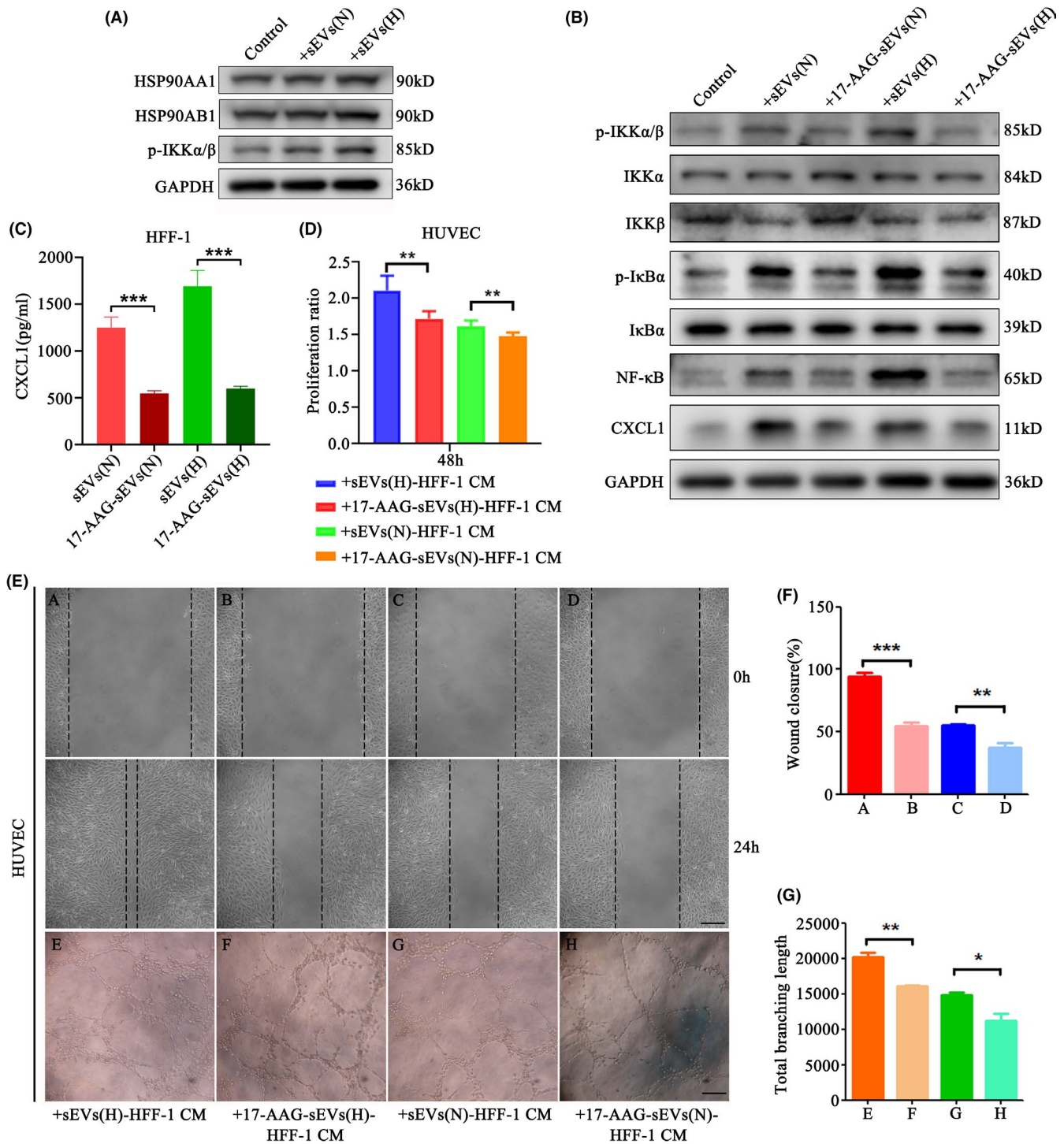


FIGURE 5 Melanoma-derived small extracellular vesicles (sEVs) activate the IKK/IKB/NF-κB/CXCL1 axis and enhance the proangiogenic capability of cancer-associated fibroblasts (CAFs) by delivering the HSP90/p-IKKα/β complex. A, HSP90AA1, HSP90AB1, and p-IKKα/β levels in HFF-1 cells were detected after normoxic and hypoxic A375-derived sEV stimulation. GAPDH was used as the internal control. N, normoxic; H, hypoxic. B, Pretreating sEVs with 17-AAG reduced p-IKKα/β, p-IκBα, NF-κB, and CXCL1 levels in sEV-treated HFF-1 cells. C, Pretreating sEVs with 17-AAG reduced CXCL1 secretion in sEV-treated HFF-1 cells. HUVEC proliferation (D), migration (E, F), and tube formation (E, G) were significantly inhibited when sEVs were pretreated with 17-AAG. Scale bar: 50 μm. Independent experiments were performed in triplicate. *P < .05, **P < .01, ***P < .001; Student's *t* tests. Values represent means ± SEM

progression in vitro and in vivo (Figure 7). Furthermore, targeting chaperone HSP90 might be a potential therapeutic strategy for melanoma treatment.

Small extracellular vesicles play key roles in intercellular communication between tumor and stromal cells within the TME. By secreting sEVs, tumor cells orchestrate stromal cells to facilitate

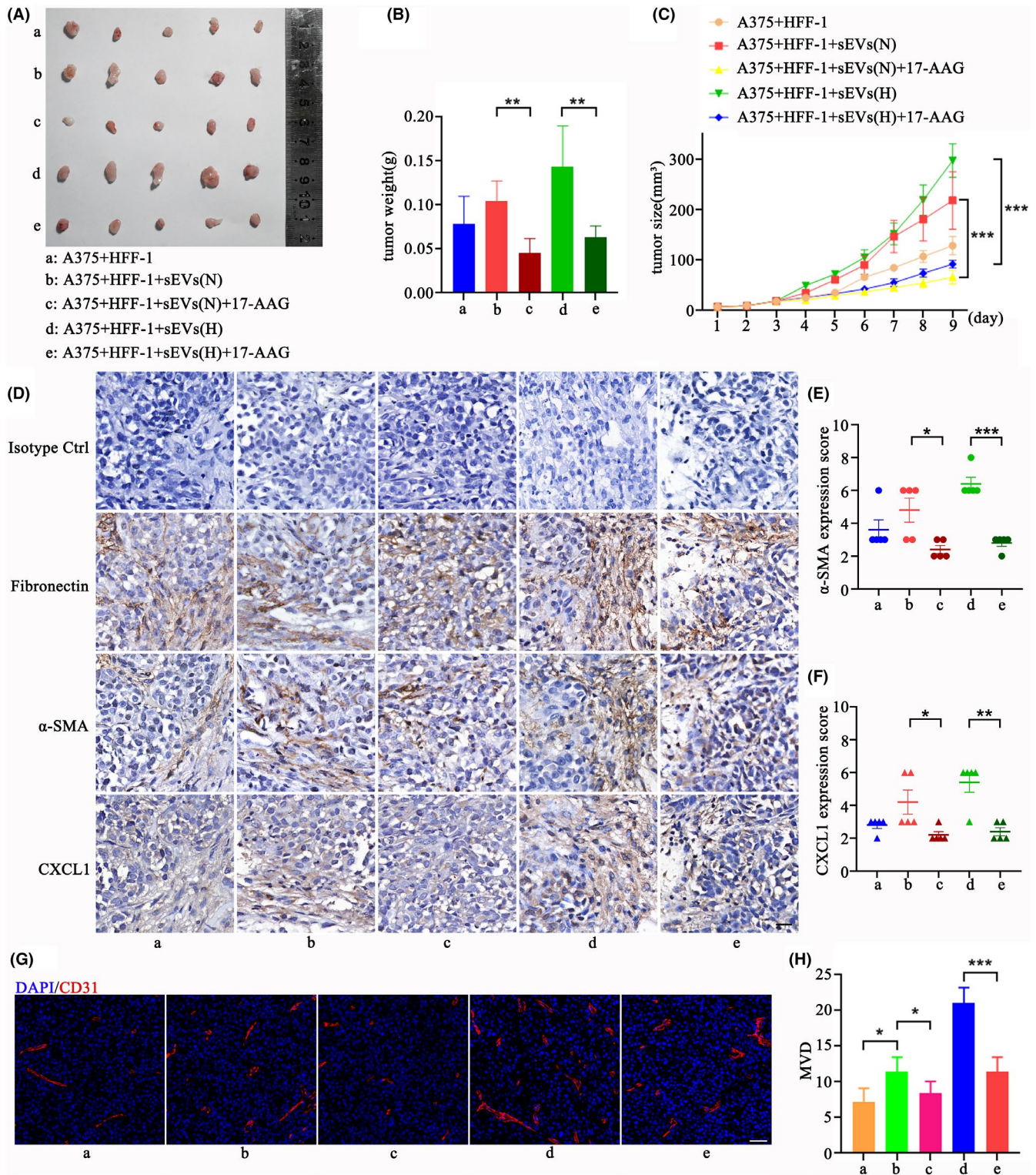


FIGURE 6 Blocking HSP90 impairs the promoting effects of small extracellular vesicles (sEVs) on melanoma angiogenesis and progression in vivo. Xenografts were extracted, photographed (A) and weighed (B). The size of xenografts was measured every day (C). The expression of fibronectin, α -SMA, and CXCL1 in xenografts was detected by immunohistochemistry (IHC) analysis (D) and quantified (E, F). Endothelial marker CD31 in xenografts was detected by fluorescent microscope, and microvessel density (MVD) of xenografts was quantified (G, H). N, normoxic; H, hypoxic. Scale bar: 20 μ m (D), 100 μ m (G). Independent experiments were performed in triplicate. * $P < .05$, ** $P < .01$, *** $P < .001$; Student's t tests. Values represent means \pm SEM

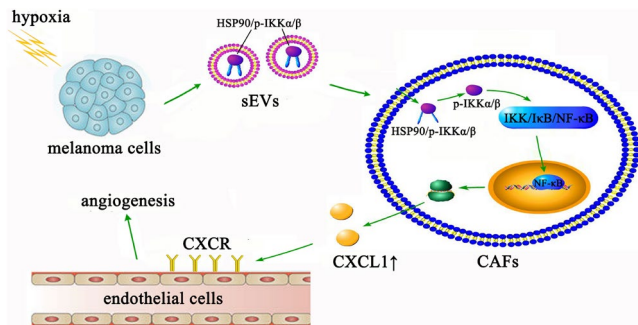


FIGURE 7 Hypoxic stress could promote enrichment of chaperone HSP90 and its client protein p-IKK α / β in melanoma-derived small extracellular vesicles (sEVs). Small extracellular vesicles derived from melanoma cells, especially hypoxic melanoma cells, could activate the IKK/ ι κB/NF- κ B signaling pathway and promote CXCL1 expression in cancer-associated fibroblasts (CAFs). Elevated CXCL1 secretion from CAFs was able to promote tumor angiogenesis. CXCR, CXCL receptor

tumor progression. Within solid tumors, hypoxia could promote sEV secretion from tumor cells and alter the cargos of sEVs. These hypoxic sEVs played critical roles in tumor progression and TME regulation.^{13,14} We had found that melanoma-derived exosomes could transfer miR-155-5p to trigger the proangiogenic switch of CAFs.⁵ However, the effects of hypoxic melanoma-derived sEVs on CAF phenotype modulation were still elusive. In this study, we found that hypoxic melanoma-derived sEVs were able to enhance the proangiogenic capability of CAFs in vitro and promote tumor angiogenesis and progression in vivo. As a major component of the TME, CAFs could promote tumor angiogenesis by secreting several proangiogenic factors.^{5,15,16} The proangiogenic switch of CAFs could be induced by cytokines and EVs secreted from tumor cells.^{5,17} However, how hypoxic tumor cell-secreted sEVs enhance the proangiogenic capability of CAFs was still unclear. Here, we found that hypoxic melanoma-derived sEVs significantly improved CXCL1 expression and secretion in CAFs, and blocking CXCL1 in the CM of CAFs apparently inhibited HUVEC proliferation, migration, and tube formation. CXCL1 is one of the crucial contributors to melanoma progression and a potent regulator of angiogenesis.^{18,19} In this study, we found that the proangiogenic capability enhancement of CAFs was due to CXCL1 expression improvement induced by hypoxic melanoma-derived sEVs.

The NF- κ B signaling pathway plays critical roles in inflammation regulation and hypoxic response.¹⁰ Here, we found that melanoma cell-derived sEVs upregulated CXCL1 expression in CAFs through the IKK/ ι κB/NF- κ B signaling pathway, and blocking the IKK/ ι κB/NF- κ B signaling pathway remarkably attenuated the proangiogenic capability of CAFs. Previous studies had found that tumor cell-derived EVs could transfer M2 pyruvate kinase, latent membrane protein 1, and integrin beta-like 1 into CAFs, leading to the persistent activation of the NF- κ B signaling pathway in CAFs.²⁰⁻²³ However, the mechanisms underlying NF- κ B signaling activation in CAFs induced by melanoma-derived sEVs remained unclear. In this

study, we discovered that hypoxia could promote the enrichment of the HSP90/p-IKK α / β complex in melanoma-derived sEVs. Transfer of the HSP90/p-IKK α / β complex to CAFs by sEVs significantly activated the IKK/ ι κB/NF- κ B/CXCL1 axis in CAFs.

HSP90 is aberrantly upregulated in varieties of tumors including melanoma.²⁴ As a chaperone, HSP90 takes part in client protein folding, trafficking, and degradation and plays key roles in signal transduction and intracellular communication.^{25,26} Besides, the complexes of HSP90 and its client proteins could be transferred to stromal cells by tumor-derived EVs.²⁷ In this study, we found that HSP90 bonded p-IKK α / β , and the HSP90/p-IKK α / β complex could be delivered to fibroblasts by melanoma-derived sEVs. Pretreating sEVs with 17-AAG remarkably decreased the load of p-IKK α / β in normoxic and hypoxic sEVs and attenuated the promoting effects of sEVs on IKK/ ι κB/NF- κ B signaling activation and CXCL1 expression in CAFs. Targeting HSP90 might be a promising strategy for oncotherapy. Combination therapy with HSP90 inhibitors prominently elevated the antitumor efficacy of antitumor agents.²⁸⁻³⁰ Targeting HSP90 could inhibit tumor proliferation, angiogenesis, and drug resistance³¹⁻³³ and reduce contractility and motility of CAFs.³⁴ In this study, pretreating sEVs with 17-AAG obviously reduced the proangiogenic capability of CAFs in vitro. In an in vivo study, 17-AAG inhibited tumor growth and reduced α -SMA and CXCL1 expressions in fibroblasts within the TME. Moreover, 17-AAG remarkably inhibited angiogenesis in the tumor masses. A previous study found that HNSCC cells secreted TGF- β and miR-192/215-rich sEVs to promote CAF-like differentiation. High levels of miR-192/215-family miRNAs in HNSCC sEVs targeted Caveolin-1 and inhibited TGF- β /SMAD signaling, leading to CAF-like differentiation of the fibroblasts.¹⁴ In our in vivo study, the group with hypoxic sEV injection exhibited a high level of α -SMA staining, while 17-AAG treatment groups showed significantly lower levels of α -SMA staining. It suggested that HSP90 in sEVs might play an important role in CAF differentiation and deserves further investigation.

However, there were some defects in this study. Firstly, more cell lines and primary cells needed to be enrolled in this study. Secondly, technological loss of sEVs during sample preparation for RNA-seq analysis made the results undesirable. Therefore, better EV preparation methods are required for further studies. Notably, the proteomic analysis of sEVs showed that HSP90 was at a higher level in high-metastatic melanoma-derived sEVs. Therefore, further studies should explore the roles of HSP90 in melanoma metastasis.

In summary, hypoxia could promote the enrichment of the HSP90/p-IKK α / β complex in melanoma-derived sEVs, and the transfer of HSP90/p-IKK α / β to CAFs by sEVs could activate the IKK/ ι κB/NF- κ B signaling pathway and promote CXCL1 expression and secretion in CAFs, which led to melanoma angiogenesis and progression. These findings deepen the understanding of hypoxic response in melanoma progression and provide potential targets for melanoma treatment.

ACKNOWLEDGEMENTS

The authors appreciate the great help of Prof Yaoting Ji, Dr Hui Zhao, and Dr Yuming Xu (School and Hospital of Stomatology, Wuhan

University). This study was supported by the National Natural Science Foundation of China (grant number: 81672666; 81972547 to Zhengjun Shang) and the Fundamental Research Funds for the Central Universities (grant number: 2042020kf0176 to Xiaocheng Zhou).

DISCLOSURE

The authors have no conflict of interest.

ORCID

Hokeung Tang  <https://orcid.org/0000-0003-3284-2061>

Xinyue Luo  <https://orcid.org/0000-0003-0556-8773>

Zhe Shao  <https://orcid.org/0000-0003-2357-3760>

REFERENCES

- Davis LE, Shalin SC, Tackett AJ. Current state of melanoma diagnosis and treatment. *Cancer Biol Ther.* 2019;20(11):1366-1379. doi:10.1080/15384047.2019.1640032
- Bussard KM, Mutkus L, Stumpf K, Gomez-Manzano C, Marini FC. Tumor-associated stromal cells as key contributors to the tumor microenvironment. *Breast Cancer Res.* 2016;18(1):84. doi:10.1186/s13058-016-0740-2
- Gargiulo E, Paggetti J, Moussay E. Hematological malignancy-derived small extracellular vesicles and tumor microenvironment: the art of turning foes into friends. *Cells.* 2019;8(5):511. doi:10.3390/cells8050511
- Bertolini I, Ghosh JC, Kossenkov AV, et al. Small extracellular vesicle regulation of mitochondrial dynamics reprograms a hypoxic tumor microenvironment. *Dev Cell.* 2020;55(2):163-177.e6. doi:10.1016/j.devcel.2020.07.014
- Zhou X, Yan T, Huang C, et al. Melanoma cell-secreted exosomal miR-155-5p induce proangiogenic switch of cancer-associated fibroblasts via SOCS1/JAK2/STAT3 signaling pathway. *J Exp Clin Cancer Res.* 2018;37(1):242. doi:10.1186/s13046-018-0911-3
- Zhao X-P, Wang M, Song Y, et al. Membrane microvesicles as mediators for melanoma-fibroblasts communication: Roles of the VCAM-1/VLA-4 axis and the ERK1/2 signal pathway. *Cancer Lett.* 2015;360(2):125-133. doi:10.1016/j.canlet.2015.01.032
- Wang Y, Liu J, Jiang Q, et al. Human adipose-derived mesenchymal stem cell-secreted CXCL1 and CXCL8 facilitate breast tumor growth by promoting angiogenesis. *Stem Cells (Dayton, Ohio).* 2017;35(9):2060-2070. doi:10.1002/stem.2643
- Vries MH, Wagenaar A, Verbruggen SE, et al. CXCL1 promotes arteriogenesis through enhanced monocyte recruitment into the pericollateral space. *Angiogenesis.* 2015;18(2):163-171. doi:10.1007/s10456-014-9454-1
- Wang D, Wang H, Brown J, et al. CXCL1 induced by prostaglandin E2 promotes angiogenesis in colorectal cancer. *J Exp Med.* 2006;203(4):941-951. doi:10.1084/jem.20052124
- Korbecki J, Kojder K, Kapczuk P, et al. The Effect of Hypoxia on the Expression of CXC Chemokines and CXC Chemokine Receptors-A Review of Literature. *Int J Mol Sci.* 2021;22(2):843. doi:10.3390/ijms22020843
- Szklarczyk D, Gable AL, Nastou KC, et al. The STRING database in 2021: customizable protein-protein networks, and functional characterization of user-uploaded gene/measurement sets. *Nucleic Acids Res.* 2021;49(D1):D605-d612. doi:10.1093/nar/gkaa1074
- Broemer M, Krappmann D, Scheidereit C. Requirement of Hsp90 activity for I κ B kinase (IKK) biosynthesis and for constitutive and inducible IKK and NF- κ B activation. *Oncogene.* 2004;23(31):5378-5386. doi:10.1038/sj.onc.1207705
- Kumar A, Deep G. Exosomes in hypoxia-induced remodeling of the tumor microenvironment. *Cancer Lett.* 2020;488:1-8. doi:10.1016/j.canlet.2020.05.018
- Zhu G, Cao B, Liang X, et al. Small extracellular vesicles containing miR-192/215 mediate hypoxia-induced cancer-associated fibroblast development in head and neck squamous cell carcinoma. *Cancer Lett.* 2021;506:11-22. doi:10.1016/j.canlet.2021.01.006
- Orimo A, Gupta PB, Sgroi DC, et al. Stromal fibroblasts present in invasive human breast carcinomas promote tumor growth and angiogenesis through elevated SDF-1/CXCL12 secretion. *Cell.* 2005;121(3):335-348. doi:10.1016/j.cell.2005.02.034
- Crawford Y, Kasman I, Yu L, et al. PDGF-C mediates the angiogenic and tumorigenic properties of fibroblasts associated with tumors refractory to anti-VEGF treatment. *Cancer Cell.* 2009;15(1):21-34. doi:10.1016/j.ccr.2008.12.004
- Li Y, Fang WB, Mafuvadze B, et al. TGF- β negatively regulates CXCL1 chemokine expression in mammary fibroblasts through enhancement of Smad2/3 and suppression of HGF/c-Met signaling mechanisms. *PLoS One.* 2015;10(8):e0135063. doi:10.1371/journal.pone.0135063
- Caunt M, Hu L, Tang T, Brooks PC, Ibrahim S, Karpatkin S. Growth-regulated oncogene is pivotal in thrombin-induced angiogenesis. *Can Res.* 2006;66(8):4125-4132. doi:10.1158/0008-5472.can-05-2570
- Botton T, Puissant A, Cheli Y, et al. Ciglitazone negatively regulates CXCL1 signaling through MITF to suppress melanoma growth. *Cell Death Differ.* 2011;18(1):109-121. doi:10.1038/cdd.2010.75
- Su S, Chen J, Yao H, et al. CD10(+)/GPR77(+) cancer-associated fibroblasts promote cancer formation and chemoresistance by sustaining cancer stemness. *Cell.* 2018;172(4):841-856.e16. doi:10.1016/j.cell.2018.01.009
- Gu J, Li X, Zhao L, et al. The role of PKM2 nuclear translocation in the constant activation of the NF- κ B signaling pathway in cancer-associated fibroblasts. *Cell Death Dis.* 2021;12(4):291. doi:10.1038/s41419-021-03579-x
- Wu X, Zhou Z, Xu S, et al. Extracellular vesicle packaged LMP1-activated fibroblasts promote tumor progression via autophagy and stroma-tumor metabolism coupling. *Cancer Lett.* 2020;478:93-106. doi:10.1016/j.canlet.2020.03.004
- Ji Q, Zhou L, Sui H, et al. Primary tumors release ITGBL1-rich extracellular vesicles to promote distal metastatic tumor growth through fibroblast-niche formation. *Nat Commun.* 2020;11(1):1211. doi:10.1038/s41467-020-14869-x
- Fukuyo Y, Hunt CR, Horikoshi N. Geldanamycin and its anticancer activities. *Cancer Lett.* 2010;290(1):24-35. doi:10.1016/j.canlet.2009.07.010
- Mbofung RM, McKenzie JA, Malu S, et al. HSP90 inhibition enhances cancer immunotherapy by upregulating interferon response genes. *Nat Comm.* 2017;8(1):451. doi:10.1038/s41467-017-00449-z
- Biebl M, Buchner J. Structure, function, and regulation of the Hsp90 Machinery. *Cold Spring Harbor Perspect Biol.* 2019;11(9):a034017. doi:10.1101/cshperspect.a034017
- Ma S, McGuire MH, Mangala LS, et al. Gain-of-function p53 protein transferred via small extracellular vesicles promotes conversion of fibroblasts to a cancer-associated phenotype. *Cell Rep.* 2021;34(6):108726. doi:10.1016/j.celrep.2021.108726
- Zhang Y, Ware MB, Zaidi MY, et al. Heat shock protein-90 inhibition alters activation of pancreatic stellate cells and enhances the efficacy of PD-1 blockade in pancreatic cancer. *Mol Cancer Ther.* 2021;20(1):150-160. doi:10.1158/1535-7163.mct-19-0911
- Calero R, Morchon E, Martinez-Argudo I, Serrano R. Synergistic anti-tumor effect of 17AAG with the PI3K/mTOR inhibitor NVP-BE235 on human melanoma. *Cancer Lett.* 2017;406:1-11. doi:10.1016/j.canlet.2017.07.021

30. Eroglu Z, Chen YA, Gibney GT, et al. Combined BRAF and HSP90 inhibition in patients with unresectable BRAFV600E-mutant melanoma. *Clin Cancer Res.* 2018;24(22):5516-5524. doi:10.1158/1078-0432.ccr-18-0565
31. Hsieh C-C, Shen C-H. The potential of targeting P53 and HSP90 Overcoming Acquired MAPKi-resistant melanoma. *Curr Treat Options Oncol.* 2019;20(3):22. doi:10.1007/s11864-019-0622-9
32. Kaur G, Belotti D, Burger AM, et al. Antiangiogenic properties of 17-(dimethylaminoethylamino)-17-demethoxygeldanamycin: an orally bioavailable heat shock protein 90 modulator. *Clin Cancer Res.* 2004;10(14):4813-4821. doi:10.1158/1078-0432.ccr-03-0795
33. Solit DB, Zheng FF, Drobnjak M, et al. 17-Allylamino-17-demethoxygeldanamycin induces the degradation of androgen receptor and HER-2/neu and inhibits the growth of prostate cancer xenografts. *Clin Cancer Res.* 2002;8(5):986-993.
34. Henke A, Franco O, Stewart G, et al. Reduced contractility and motility of prostatic cancer-associated fibroblasts after inhibition of

heat shock protein 90. *Cancers.* 2016;8(9):77. doi:10.3390/cancers8090077

SUPPORTING INFORMATION

Additional supporting information may be found in the online version of the article at the publisher's website.

How to cite this article: Tang H, Zhou X, Zhao X, et al. HSP90/IKK-rich small extracellular vesicles activate pro-angiogenic melanoma-associated fibroblasts via the NF- κ B/CXCL1 axis. *Cancer Sci.* 2022;113:1168-1181. doi:[10.1111/cas.15271](https://doi.org/10.1111/cas.15271)